ELSEVIER

Contents lists available at ScienceDirect

Advanced Powder Technology

journal homepage: www.elsevier.com/locate/apt



Original Research Paper

Orange peel ash coated Fe₃O₄ nanoparticles as a magnetically retrievable catalyst for glycolysis and methanolysis of PET waste



Samson Lalhmangaihzuala ^{a,b,1}, ZT Laldinpuii ^{a,b,1}, Vanlalngaihawma Khiangte ^{a,b}, Gospel Lallawmzuali ^{a,c}, Thanhmingliana ^a, K. Vanlaldinpuia ^{a,*}

- ^a Department of Chemistry, Mizoram University, Pachhunga University College Campus, Aizawl, 796001, Mizoram, India
- ^b Department of Chemistry, Mizoram University, Tanhril, Aizawl, 796004, Mizoram, India
- ^c Department of Environmental Science, Mizoram University, Tanhril, Aizawl, 796004, Mizoram, India

ARTICLE INFO

Article history: Received 16 August 2022 Received in revised form 18 April 2023 Accepted 27 April 2023

Keywords: Nanoparticles Heterogeneous catalyst Glycolysis Methanolysis PET waste recycling

ABSTRACT

Chemical recycling of PET offers the process of recovering virgin grade raw materials that can be reprocessed to produce an intact polymeric material or other valuable products. In the current study, we investigate the advantages of exercising biowaste derived orange peel ash (OPA) magnetic nano-catalyst, OPA@Fe₃O₄ as a green and reusable heterogeneous solid catalyst for glycolytic and methanolytic degradation of PET waste. The composition and physical features of the prepared catalyst were studied and analyzed using various techniques. Under the optimized condition, the catalyst was able to obtain an excellent bis(2-hydroxyethyl) terephthalate (BHET) and dimethyl terephthalate (DMT) yield with 100% PET conversion. Moreover, the catalyst was able to be recycled for ten consecutive runs for both processes without a significant reduction in the yield of the reaction, addressing the possible implementation of the catalyst for industrial purposes.

© 2023 The Society of Powder Technology Japan. Published by Elsevier B.V. and The Society of Powder Technology Japan All rights reserved.

1. Introduction

The extensive amount of plastic production distinctly demonstrated their gaining of popularity on a global scale. During the last six decades, production of plastic materials dominated the manufacturing industry and greatly surpassed almost all other manmade materials.[1] Once dubbed as 'materials of 1,000 uses', the use of plastics traverses almost every sector, from clothing to automotive industry as well as making ends meet from medical to electronics equipment.[2,3] Since its commercial production in 1950 s, more than 8.3 billion tons of plastic has been produced worldwide. [4] In 2012 alone, 280 million tons of plastic was generated globally and it is estimated that the global overall plastic production will reach 33 billion tons by 2050 if the ongoing consumption rates continue.[5] Excellent resistance to air, water and chemicals, low cost and ease of manufacturing, high strength-to-weight ratio and easy handling of the material enhance their increasing domination in the consumer marketplace and has permeated nearly every aspect of our day-to-day life.[1,4] And one amazing feature

of plastic is that its utilization can be easily differentiated based on its design, each one with a specific characteristic to make them idyllic for each purpose. However, despite its relentless production and applications, lack of a proper dumping system has generated a huge level of plastic pollution, and consequently, is having an adverse effect on the environment.[6] To combat against these massive accumulations of plastic waste in our surrounding, roadmaps for an innovative reduction of plastics footprints were developed using various methods,[7] such as primary recycling, secondary or mechanical recycling, tertiary or chemical recycling and quaternary recycling (recovery of energy through pyrolysis or incineration). Among these, the chemical recycling of plastic waste occupies the top of the waste disposal pyramid, but the current recycling tool box has immensely adorned a secondary or mechanical form of reprocessing technique rather than the tertiary or chemical form of treatment available.[7,8] Unfortunately, continuous reprocessing of the material through physical process has caused certain degree of chemical identity alteration, such as change in coloration or decrease in molecular weight of the product, and thus the technique is often referred to as 'downgrading' or 'downcycling' process.[2,9] Right now, tertiary or chemical recycling is the only method which conforms to the principle of green

^{*} Corresponding author.

E-mail address: mapuiakhiangte@pucollege.edu.in (K. Vanlaldinpuia).

¹ Equal contribution for the first two authors.

chemistry and promises an attractive long-term strategy for obtaining high-quality monomeric feedstocks.[10].

Nearly 40% of the total polymers synthesized were employed in the packaging industry, of which polyethylene terephthalate (PET or PETE) occupies the majority.[4] It is one of the most flexible polymers that is predominantly used in the production of packaging bottles for mineral water and carbonated soft drinks, food packaging, transparent films, and glass-replacement in some applications.[11,12] It is also the easiest and most common plastic to recycle and hence, in recent years, the chemical recycling of PET waste has attracted numerous attention among researchers. It is usually performed *via* methanolysis, glycolysis, hydrolysis, aminolysis and ammonolysis through the cleavage of ester linkages at the polyester chain by nucleophilic reagents such as methanol, glycols, water or hydroxide, amines and ammonia.[2,12].

Among the chemical recycling techniques mentioned above, glycolvsis is the most common method of PET waste recycling and the least expensive procedure in terms of capital. It is a kind of endothermic, solvolytic chain cleavage reaction, where molecular degradation of PET polyester was performed using glycols and a transesterification catalyst. During the course of reaction, the ester binding broke and it was replaced with hydroxyl endings to generate bis(2-hydroxyethyl) terephthalate (BHET) and its oligomers at a relatively high temperature (180–240 °C).[12–14] Prior studies have shown that several catalysts such as metal derivatives, 15-19] zeolites,[20] ionic liquids[21–29] and organocatalysts[9,30,31] powered this method of depolymerization of PET waste. Meanwhile, methanolysis, another chemical pathway for the degradation of PET resin using methanol at a very high temperature and pressure yielded dimethyl terephthalate (DMT) and ethylene glycol (EG) as the main products. The key benefits of methanolysis include the simplicity with which the monomer, DMT, can be purified; the ease with which ethylene glycol and methanol can be recovered; and the relatively high tolerance to impurities, allowing for the treatment and recycling of low-quality feedstocks. Different approaches to methanolysis were studied[13,32-35] and reported that the process could undergo a facile depolymerization reaction under supercritical conditions or in the presence of catalysts at a slightly reduced temperature. Several examples of methanolysis using catalysts such as divalent metals, hydroxides of alkali earth metals, lead acetate and aluminium triisopropoxide were demonstrated.[13,35-39] However, high cost of the procedure, low selectivity of the desired products and high toxicity of the catalysts are some of the limiting factors of the described protocols. Hence, the search for a novel transesterification catalyst, which is ecofriendly and cost-effective for promoting efficient and effective recycling techniques for PET is crucial and is still an area of active research. Recently, in an attempt to reduce the cost of PET recycling techniques, we have investigated the use of biomass waste-derived ashes as recyclable heterogeneous catalysts for PET waste recycling. [40–43] Though the processes were simple and efficient, giving high selectivity of the monomeric feedstocks, the catalysts could be recycled for up to 5 cycles only, which could hinder its applicability at the industrial scale. In this present study, we have reported the use of orange peel ash (OPA) coated magnetic nanoparticles as an efficient, easily recoverable heterogeneous catalyst for PET waste depolymerization.

To this day, nanostructured magnetic iron oxide materials have been exploited in a broad range of applications spreading from nano-sized electronic gadgets to catalysis and biomedicine.[44–46] They can be separated easily using a magnet, which diminishes the loss of catalyst as well as increases its reusability, hence, they have been utilized extensively as heterogeneous catalysts for different types of organic transformations.[47–53] There have also been some preceding reports of magnetic iron oxide nanoparticles such as γ -Fe₂O₃, Fe₃O₄ boosted multi-walled carbon nanotube, Fe₃O₄

immobilized on hexagonal boron nitride nanosheets and ionic liquid coated SiO₂@Fe₃O₄ nanoparticles employed for the depolymerization of PET waste with varying results.[54-56] However, the preparation of these catalysts usually involves complex and lengthy synthetic procedure as well as extreme reaction condition that elevates the overall expenses and narrow the environmental affinity of PET decomposition, thus eventually confines its industrial applications. To overcome these complications, the biogenic synthesis of magnetic nanoparticles using OPA was achieved, which could potentially provide cost-effective and sustainable PET waste recycling method. Inspired by the nature of this biomass derived nanocatalyst together with our previous successful implementation[40-43] of highly basic lignocellulosic biomass towards the decomposition of waste PET, glycolysis and methanolysis of PET was investigated for the first time using magnetically retrievable heterogeneous catalyst obtained from the bio-waste material extract.

2. Experimental

2.1. Materials used

Cast-off PET bottles were gathered from the streets of Aizawl, Mizoram, India. The bottles were washed repeatedly with distilled water, dried and then cut into pieces of 1 mm squares. The chemicals FeSO₄·7H₂O and anhydrous FeCl₃ were purchased from HiMedia. Ethylene glycol (EG), BHET and DMT (for reference) and methanol were obtained from Sigma- Aldrich. All chemicals were used as received unless otherwise stated.

2.2. Catalyst preparation

Oranges were purchased from street vendors in Aizawl, Mizoram, India. The peels were collected, washed repeatedly with distilled water to remove any impurities and then sun dried for 3 days or in an oven at 80 °C for 10–12 hrs. The dried orange peels were burnt in open air, and the ash was collected. The ash (10 gm) was then dissolved in 100 mL deionized water and stirred using an overhead stirrer for 1 hr at 80 °C to extract the basic portions from the peels. The mixture was filtered, and the orange peel extract was collected.

The magnetic Fe_3O_4 NPs was synthesized by following the traditional co-precipitation technique with small changes to the reported methodology.[57] A mixture of $FeSO_4 \cdot 7H_2O$ (5 mmol) and $FeCl_3$ (10 mmol) was added to 100 mL of deionized water which was pre-heated at 90 °C with vigorous stirring. To this, 20 mL of the OPA extract was added dropwise until the solution changed from brownish color to dark brown. Then a small amount of 1 M ammonia solution was added dropwise till the color of the solution changed from dark brown to fully dark. The prepared Fe_3O_4 NPs was allowed to settle, the solution was decanted, and the solid part at the bottom was collected. The magnetite nanoparticle was mixed with 50 mL of orange peel extract and then stirred at room temperature for another 30 min. The water was evaporated using a rotary evaporator and the dried OPA coated nanocatalyst was collected and stored in a vacuum at room temperature.

2.3. Catalyst characterization

The prepared catalyst, $OPA@Fe_3O_4$ was well characterized using various techniques such as X-ray fluorescence (XRF), X-ray photoelectron spectroscopy (XPS), Energy-dispersive X-ray spectroscopy (EDAX or EDX), Fourier-transform infrared spectroscopy (FTIR), X-ray diffraction (XRD), Thermogravimetric analysis (TGA), Scanning Electron microscope (SEM), High-resolution transmission electron microscopy (HR-TEM) and Brunauer Emmett Teller (BET) analysis.

X-ray fluorescence analysis was performed to investigate the particular composition of the catalyst using PANalytical, Axios mAX. The FT-IR spectra recording was performed on Spectrum BX FT-IR using KBr disks $(\upsilon_{max}$ in cm $^{-1})$. For examining the crystalline composition of the catalyst, Powder X-ray diffraction (XRD) was recorded on Xpert MPD. Surface morphology of the solid catalysts was analyzed using Scanning Electron Microscope (SEM) and its chemical composition was recorded on JSM-6360 and ESEM EDAX XL-30 instruments. Transmission Electron Microscope (TEM) image was obtained on JEM-2100, 200 kV instrument. Thermal stability of the catalyst was also studied using Perkin Elmer, TGA 4000 under nitrogen atmosphere. Surface area of the catalyst was recorded using BET analysis on Quanta chrome Nova-1000 surface area and porosity analyzer. XPS analysis was performed on a Physical Electronics, model no. PHI 5000 VersaProbe III instrument.

2.4. Procedure for glycolysis of PET waste

PET glycolysis reaction was performed in a two-necked 100 mL round bottom flask fitted with a thermometer and a condenser. The round bottom flask was charged with 2.5 mmol of PET flakes, 4 wt% of OPA@Fe₃O₄ and 2.25 mmol of EG, and then it was dipped in an oil bath pre-heated at 190 °C. The reaction was carried out at the predetermined temperature under atmospheric pressure for 1.5 hrs. After the disappearance of PET flakes, which was used as a visual indicator for completion of the reaction, the catalyst was separated using an external magnet. The reaction mixture was filtered and then washed with hot water (100 mL) to remove the water-insoluble part. The filtrate was concentrated to about 40 mL using a rotary evaporator and then stored in a refrigerator at 2 °C overnight. Finally, a crystallized BHET product separates out, which was filtered, dried and then weighed. The yield percentage of the BHET monomer was calculated using the following equation:

$$\mbox{Yield of BHET monomer } (\%) = \frac{\mbox{\it ActualyieldofBHETmonomer}}{\mbox{\it TheoreticalyieldofBHET}} \mbox{\it x100} \end{matrix} \label{eq:actualyieldofBHET}$$

2.5. Procedure for methanolysis of PET waste

Methanolysis of PET was also performed with 4 wt% of OPA@Fe $_3$ O $_4$ catalyst in a Shilpent Teflon Lined Hydrothermal Autoclave reactor loaded with 2.5 mmol of PET flakes and 49 M equivalents of methanol (5 mL) in an oil bath at a temperature of 200 °C for 1 hr reaction time. After the reaction was completed, the catalyst was recovered using external magnet and the reaction mixture was filtered and washed with 40 mL of hot methanol. The mixture was allowed to cool down to room temperature and then placed in a refrigerator at 2 °C for 4 hrs, where a crystallized DMT crystal out, which was filtered, dried and weighed. The filtrate was then concentrated under reduced pressure to recover methanol and ethylene glycol. The white crystalline residue was collected and characterized using HPLC and NMR. The yield % of the recrystallized DMT was calculated using the following equations:

$$Yield \ of \ DMT \ monomer \ (\%) \ = \ \frac{\textit{ActualyieldofDMTmonomer}}{\textit{TheoreticalyieldofDMT}} x 100 \end{(2)}$$

2.6. Characterization of the depolymerized BHET and DMT

The BHET and DMT products obtained were analyzed using ¹H NMR and ¹³C NMR spectroscopy on Bruker, 400 MHz Avance III spectrometer. The presence of functional groups was determined

using FTIR spectra performed on Spectrum BX FT-IR, Perkin Elmer in 4000–500 cm $^{-1}$ range. HPLC (High Pressure Liquid Chromatography) was performed on Waters 1525 binary pump and Waters UV detector 2489 using Spherisorb ODS2 5 μm , 4.6 \times 250 mm analytical column at 254 nm. Methanol and water mixture at 70/30 vol fraction at a flow rate of 1 mL/minute was used as a mobile phase.

3. Result and discussion

3.1. Catalyst characterization

3.1.1. X-ray fluorescence (XRF)

XRF analysis was carried out to analyze the presence of compound oxides on the catalyst (see Supplementary Material Table S1). XRF data showed oxides of Iron (55.786%), potassium (26.17%) and sulfur (8.857%) as the major components and the presence of Na₂O, P₂O₅, MgO, SiO₂, CaO etc., was also detected in small quantities. The excessive concentration of metal oxide greatly influenced the catalyst performance in the process of PET depolymerization.[40] As a result, with response to the above assertions, coating of highly basic alkaline OPA with basic Fe₃O₄ NPs will eventually boost the basic concentration of the prepared catalyst and thereby making it perfectly suitable for the production of PET monomer.

3.1.2. X-ray photoelectron spectroscopy (XPS)

XPS technique was performed to explore the surface chemical composition of the present catalyst. From the survey spectra of the nanomaterial, presence of an element such as potassium, carbon and oxygen can be observed (Fig. 1a-d). On deconvolution of the K2p spectra, two peaks at 290.61 and 293.08 eV correspond to the existence of K₂O and K₂CO₃ of the catalyst. Likewise, the deconvoluted spectra of C1s comprise of four humps with different binding energies, where the peak at 282.76 eV is due to an adventitious carbon and peaks at 286.75 and 290.48 eV can be attributed to C-O and O-C = O bonds, respectively, indicating the occurrence of metal carbonates.[58] Also, the peak at 293.02 eV can be credited to the formation of bonds between carbon atoms and an electronegative atom within the vicinity. Similarly, the O1s spectra on deconvolution show one peak at 528.77 eV to corroborate the availability of Fe-O bond in the catalyst.[59,60].

3.1.3. X-ray crystallography (XRD)

The crystalline nature of the prepared nanocatalyst was also characterized using XRD analysis (Fig. 1e). The XRD data displayed peaks at 2θ = 32.195, 40.499, 51.484, and 66.400, which can be attributed to the presence of K_2CO_3 (JCPDS file no: 71–1466). Likewise, the occurrence of Fe_3O_4 can be confirmed by the detection of peaks at 2θ = 29.809, 35.554, 43.362, 57.109 and 62.748 (JCPDS file no: 89–0691). The presence of K_2O , CaO and CaCO $_3$ was also confirmed by the appearance of peaks at 2θ = 25.743, 28.302, 38.846, 53.763, 30.849 and 50.204 (JCPDS file no: 77–2151, 77–2176, 82–1690 and 87–1863).

3.1.4. Fourier-transform infrared spectroscopy (FTIR)

The functional group present in the catalyst was also studied by recording its FTIR spectra as shown in Fig. 1f. From analysis, the peak at around 3419 cm⁻¹ can be ascribed to the presence of moisture content adsorbed by the catalyst. Also, the peaks observed at 1646, 1391, 1119 and 886 cm⁻¹ correspond to the stretching and bending vibration of metallic carbonates present in the catalyst. [57,61,62] Besides these, the peak observed at 615 cm⁻¹ was attributed to the stretching vibration of metallic oxide.[57,63].

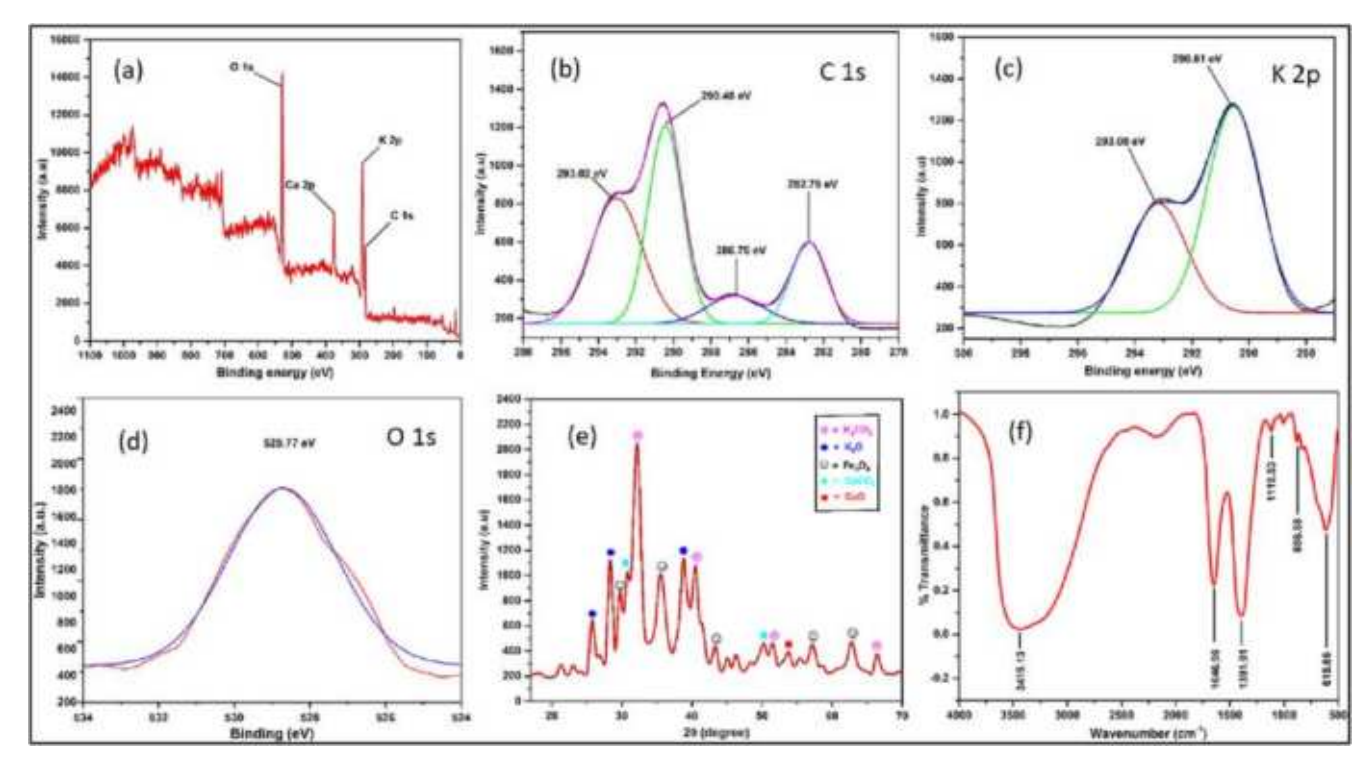


Fig. 1. (a-d) XPS analysis of OPA@Fe₃O₄, (e) XRD data of OPA@Fe₃O₄, (f) FT-IR spectrum of OPA@Fe₃O₄.

3.1.5. Energy dispersive X-ray analysis (EDX or EDAX)

EDX or EDAX analysis was further carried out to validate the data obtained from XRF as well as XPS analysis (Fig. 2a). The EDX analysis displayed K, Fe, O, etc. as the major chemical content of OPA coated Fe $_3$ O $_4$ catalyst. Thus, the EDX analysis was found to be in accordance with XRF and XPS data, and the analyzed atomic wt% of the elements was also displayed.

3.1.6. Thermogravimetric analysis (TGA)

TGA analysis was performed at a temperature ranging from 30 to 1000 °C to show the temperature at which the OPA@Fe $_3$ O $_4$ catalyst decomposed under N $_2$ atmosphere. The TGA thermogram shows the first weight reduction of 12% at about 100 °C which may be due to the loss of water molecules adsorbed by the catalyst (Fig. 2b). The further weight reduction detected at an elevated temperature might be resulted from the oxidation of the carbon content of the catalyst in the form of their oxides.[64].

3.1.7. Scanning electron microscope (SEM) and transmission electron microscope (TEM)

Surface morphology of the catalyst was also investigated by SEM analysis. Fig. 3a and 3b shows SEM image with a magnification of 10 μ m, displaying an irregular rectangular rod-like structure agglomerated to each other with a highly porous surface.

TEM analysis was also employed to investigate the structural appearance and size dimensions. From the examination, observation of a shell-like appearance confirmed the successful introduction of M–O and M–CO $_3^2$ (M = metals) on Fe $_3$ O $_4$ NPs.[57] As shown in Fig. 3c and 3d, the average nano-sized of the catalysts was observed to be ~ 10 –20 nm. In addition, the SAED (Selected area diffraction) pattern displayed the nature of the catalyst, OPA@Fe $_3$ O $_4$ to be polycrystalline, showing an indistinct boundary.

3.1.8. Brunauer-Emmett-Teller (BET)

BET analysis was used to determine the surface area, pore volume and pore diameter of OPA@Fe₃O₄ catalyst (Fig. 4a & b). It

was observed that the catalyst displayed the characteristic hysteresis loop of type H1, indicating the mesoporous identity of the catalyst.[65] BJH (Barrett, Joyner, and Halenda) method determined the pore volume to be 0.085 cc/g and pore diameter at 5.123 nm, which fulfilled the mesoporous descriptions and validated the nitrogen isotherms. Most importantly, the surface area was observed to be 31.233 m²/g. This high surface area of the nanocatalyst offered more reaction sites which may have significantly enhanced the rate of conversion.[66,67] Additionally, in contrast to our previously reported orange peel ash (OPA) and bamboo leaf ash (BLA),[40,43] the surface area of the nanocatalyst was about six times higher than the ash samples. Hence, the present catalyst was accredited to improve and upgrade recently reported OPA and BLA mediated glycolysis and methanolysis reaction.

3.2. Glycolysis reaction of PET waste

Glycolysis of PET was conducted following the reaction procedure as previously described in the experimental section. The resultant recrystallized BHET product obtained was examined by 1 H NMR and 13 C NMR spectroscopy using DMSO d_{6} as a solvent. The characteristics of aromatic proton and hydroxyl proton peaks were observed at 8.13 ppm and 4.98 ppm, respectively (Fig. 5). While the existence of peaks at 4.33 ppm and 3.73 ppm can be assigned to the presence of methylene protons of COO-C \underline{H}_{2} and C \underline{H}_{2} -OH, correspondingly. Also, the peak detected at 2.51 ppm corresponds to the triplets of DMSO. From 13 C NMR spectra, characterization of peak at δ = 165.13, 133.71, 129.48, 67.00 and 58.95 ppm were due to the presence of carbonyl, aromatic, and methylene carbons, confirming the formation of the resultant BHET product (see Supplementary Material Figure S1).

Moreover, the FTIR spectra of the BHET monomer (see Supplementary Material Figure S2) clearly showed the –OH vibration band at 3427 cm^{-1} , alkyl C–H at 2927 cm^{-1} and aromatic C–H at 1427 cm^{-1} . The intense peak observed at 1728 cm^{-1} was due to ester C = O stretching, and a strong absorption frequency at

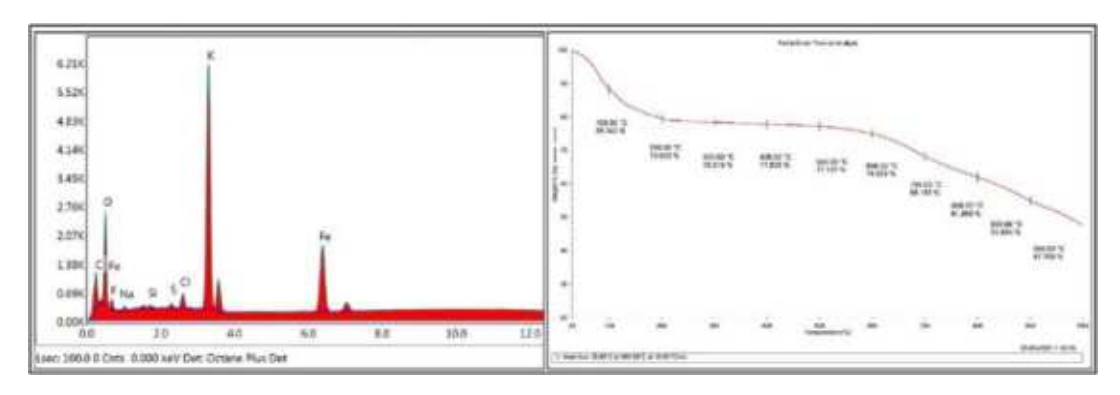


Fig. 2. (a) EDX data of OPA@Fe₃O₄, (b) TGA thermogram of OPA@Fe₃O₄.

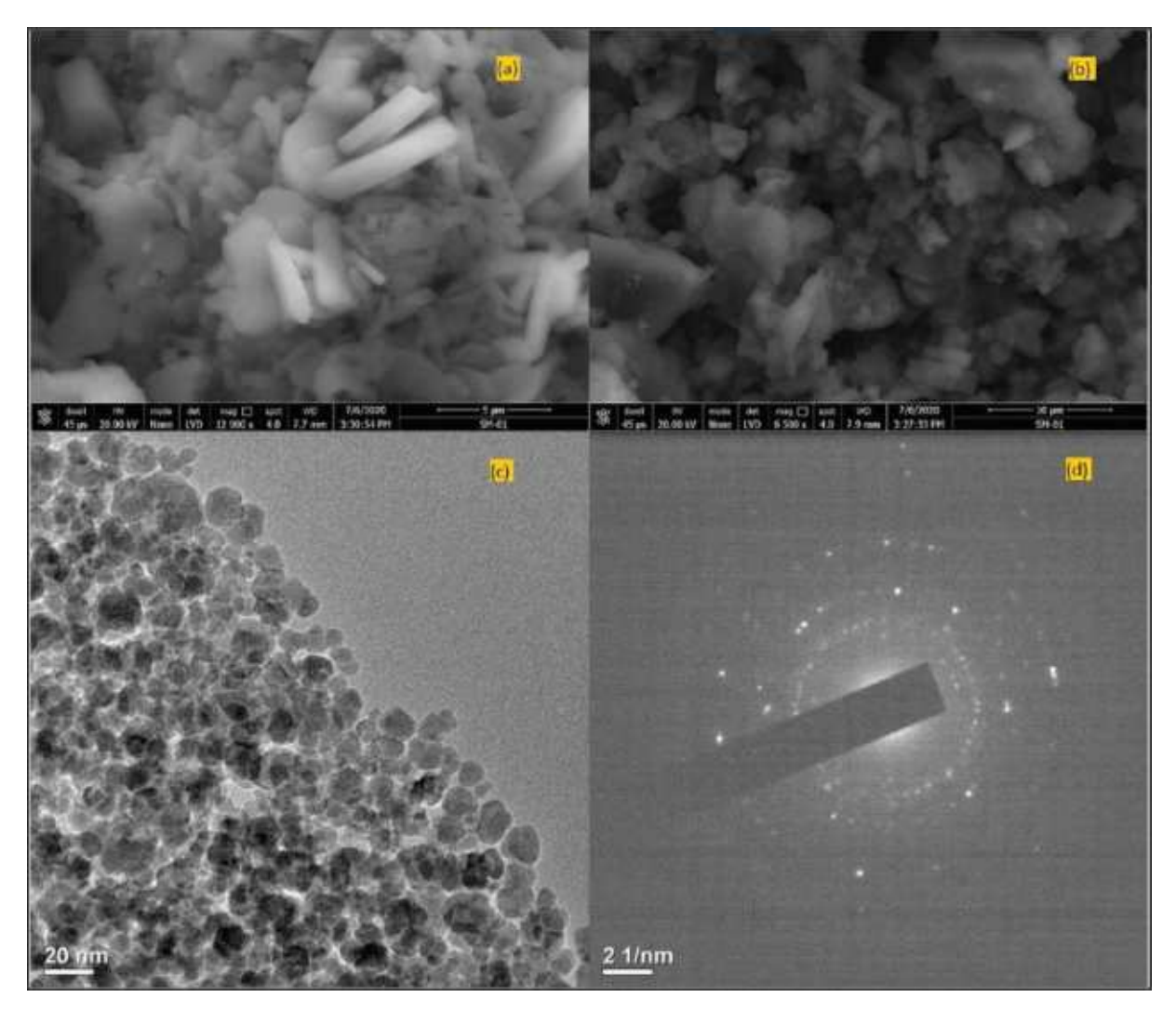


Fig. 3. SEM (a) and (b) and TEM (c) and (d) images of OPA@Fe₃O₄.

1282 cm⁻¹ and 1101 cm⁻¹ can be assigned to esters C-O bond vibration, all of which are present in BHET. Analysis of the crude product using HPLC analysis revealed the formation of products other than BHET. Peaks at a retention time of 1.858, 3.383 and 6.362 indicated the presence of ethylene glycol (EG), BHET and BHET dimer respectively (see Supplementary Material Figure S3). This was confirmed by the HPLC analysis of the commercially available EG, BHET monomer, the recrystallized product and water-insoluble part.[41].

To evaluate the experimental condition for maximum production of BHET from PET, the effects on BHET yield due to various reaction parameters were investigated in presence of OPA@Fe₃O₄.

3.2.1. Optimization of reaction time

The influence of reaction time on BHET production is shown in Fig. 6 (a). Studies were conducted by varying the duration of the reaction time from 1-3 hrs using a catalyst amount of 10 wt%, temperature of 190 °C and 16 equivalents of EG. The product

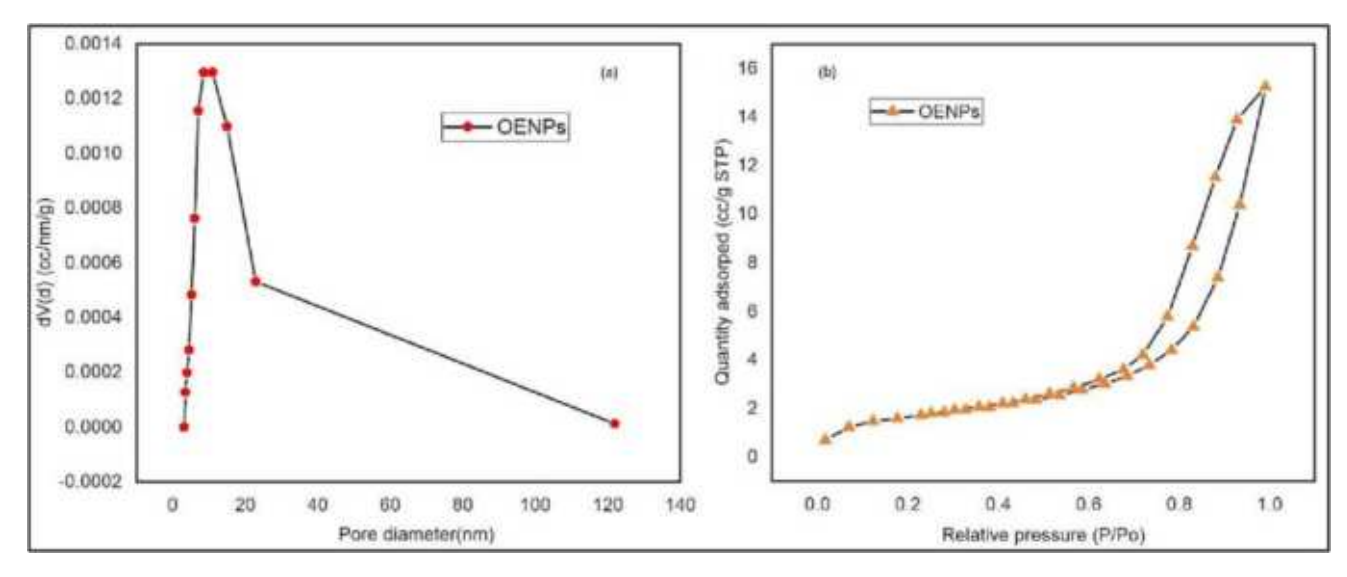


Fig. 4. (a) BJH pore size distribution of OPA@Fe₃O₄, (b) Nitrogen adsorption-desorption isotherm of OPA@Fe₃O₄.

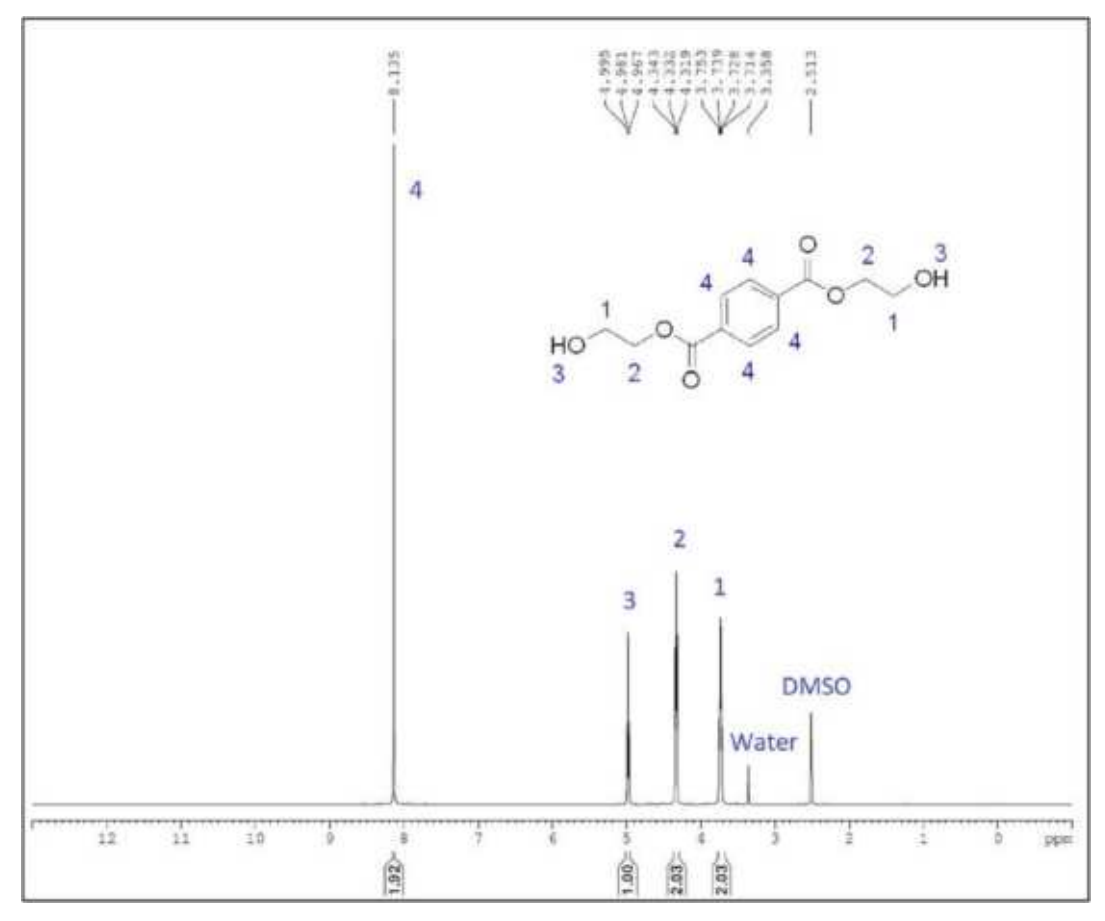


Fig. 5. ¹H NMR data of recrystallized BHET.

showed a significant improvement with increasing reaction time, and the best yield was obtained after 1.5 hrs of reaction, giving 85% BHET yield. However, allowing the reaction to run beyond 1.5 hrs results in the decreased formation of BHET as well as increased production of the water-insoluble part. This may be due to the fact that PET depolymerization is a reversible process

in which the depolymerized PET gets repolymerized into its dimer and oligomers during the process, subsequently decreasing the BHET yield.[40] As an equilibrium exists between PET monomer and its dimer and/or oligomers,[2,68] managing the optimum reaction time for PET degradation is crucial for obtaining maximum BHET yield.

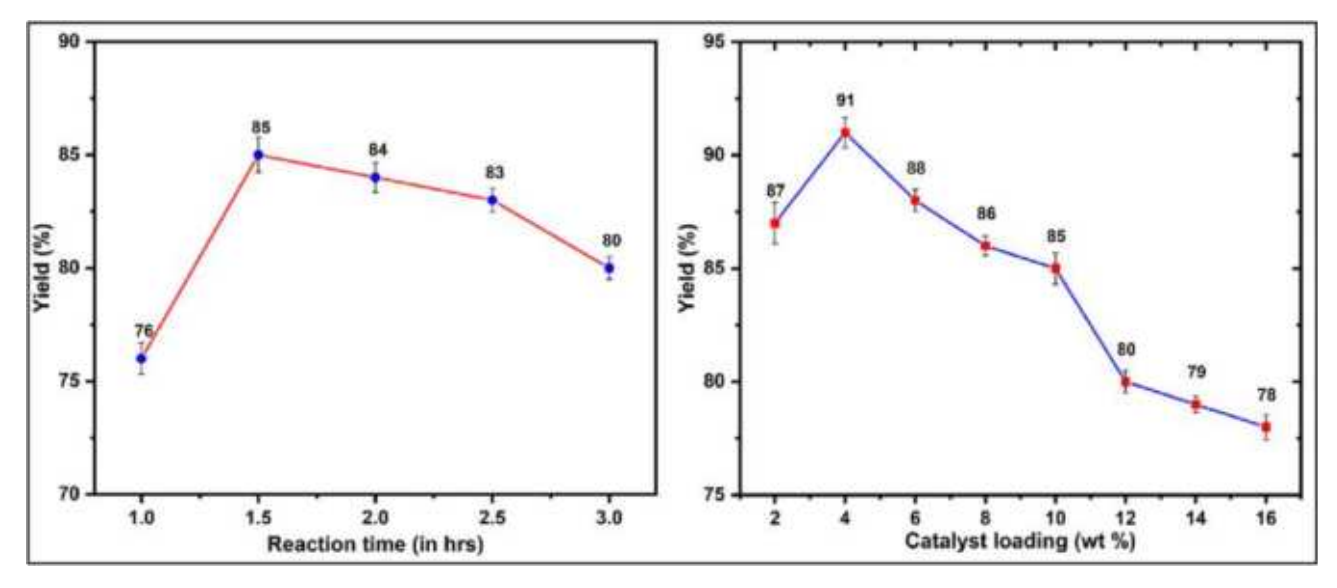


Fig. 6. (a) Optimization of the reaction time. Reaction condition: 2.5 mmol of PET flakes, 16 equivalents of EG, 10 wt% of catalyst, at 190 °C. (b) Optimization of catalyst loading. Reaction condition: 2.5 mmol of PET flakes, 16 equivalents of EG, 1.5 hrs reaction time, at 190 °C.

3.2.2. Optimization of catalyst loading

While keeping other parameters such as reagent loading, process temperature and reaction time constant at 16 equivalents, 190 °C and 1.5 hrs, respectively, the amount of catalyst loading on transesterification of PET was evaluated in the range between 2 wt% - 16 wt% (Fig. 6b). The highest BHET yield of 91% was achieved when the catalyst concentration was at 4 wt%, and further increases in the catalyst beyond the optimal concentration have lowered the percentage of BHET yield. The reason for this preliminary increase and then decreases in BHET yield is that as the number of active sites increases rapidly with an increase in the catalyst loading, the reactions advance more quickly to form the BHET product.[26,40] However, after reaching the optimal condition, the depolymerization process proceeds much faster to form BHET monomer, but the repolymerization process was also stimulated at the same time. Hence, the equilibrium shifts towards the left side of the reaction, which eventually reduces the BHET yield while improving the formation of water-insoluble products.

3.2.3. Optimization of EG loading and reaction temperature

The impact of EG loading for PET depolymerization was also investigated, and it is one of the most important factors that decide the yield of the product (Fig. 7a). This parameter was examined by carrying out the reaction at various EG loading using 4 wt% of the catalyst and a reaction time of 1.5 hrs at 190 °C. The reaction proceeded smoothly even with just 6 equivalents of EG yielding 73% of BHET, but the best result was achieved using 16 equivalents of reagent loading. Increasing the reagent loading not only decreases the production of oligomers but also greatly influences the purification and recrystallization process as the recrystallized products obtained from lower EG loading usually contain dimers and oligomers. However, further increase in the EG concentration beyond the optimal condition decreases the BHET yield, which is attributed to the reduced concentration of the catalyst in the reaction medium.[16,68].

Similarly, the process temperature also greatly affected the general outcome of the reaction (Fig. 7b). When the reaction was carried out at 180 °C, the reaction was completed after 3.5 hrs with a recrystallized product yield of 78%. But, at 200 °C, we have observed a slight decrease in BHET yield along with an increased formation of water-insoluble products.

3.2.4. Reusability of the catalyst

One of the most important features of utilizing heterogeneous catalysts is that they have the potential to be recovered and reused repeatedly for successive catalytic cycles, offering a distinct economic advantage against their homogeneous counterparts.[69,70] To test the reusability of OPA@Fe₃O₄ catalyst, glycolysis of PET was inspected under the same optimized reaction condition. After each cycle, the catalyst was removed from the crude mixture using an external magnet, washed with hot water and finally dried at 80 °C for 12 hrs. Subsequently, without further reactivation of the catalyst, the recovered catalyst was directly employed for ten consecutive runs, and as shown in Fig. 8, it was observed that an excellent BHET yield could be achieved without any considerable reduction in the production yield. However, the reaction time for complete conversion slightly increases after each catalytic cycle which may be due to partial leaching of the active sites from the catalyst during washing or consecutive reaction operations. [71,72] After ten successive catalytic cycles, the recovered catalyst was investigated using SEM, TEM, EDX and XPS analysis to determine changes in their structure and elemental compositions.

SEM and TEM analyses showed no significant changes in the morphology and particle size of the catalyst displaying an agglomerated structure with an average particle size of 15–17 nm (see Supplementary Material Figure S5). The EDX data exhibited a significant loss of potassium (K) concentration from 28.2% to 0.4% while iron (Fe) remains almost the same (see Supplementary Material Figure S6). The XPS full scan spectrum of the reused catalyst after the tenth cycle also revealed a sharp drop in the K and Ca peaks, indicating leaching of the active sites from the surface of the nanocatalyst (see Supplementary Material Figure S7).

3.2.5. Glycolysis of color PET bottles

We also examined the glycolysis of different color PET bottles using our optimized reaction condition. It was reported that color bottles usually contain acidic components which could hamper the catalytic activity of some catalysts toward PET depolymerization. [73] To our satisfaction, all the reactions were completed within 1 hr, giving an excellent yield that is almost comparable to those of clear bottles (see Supplementary Material, Table S2). Most of the pigments were also removed during the recrystallization-filtration process, and any residual color could be eliminated by adding 30 mg of activated charcoal followed by filtration.

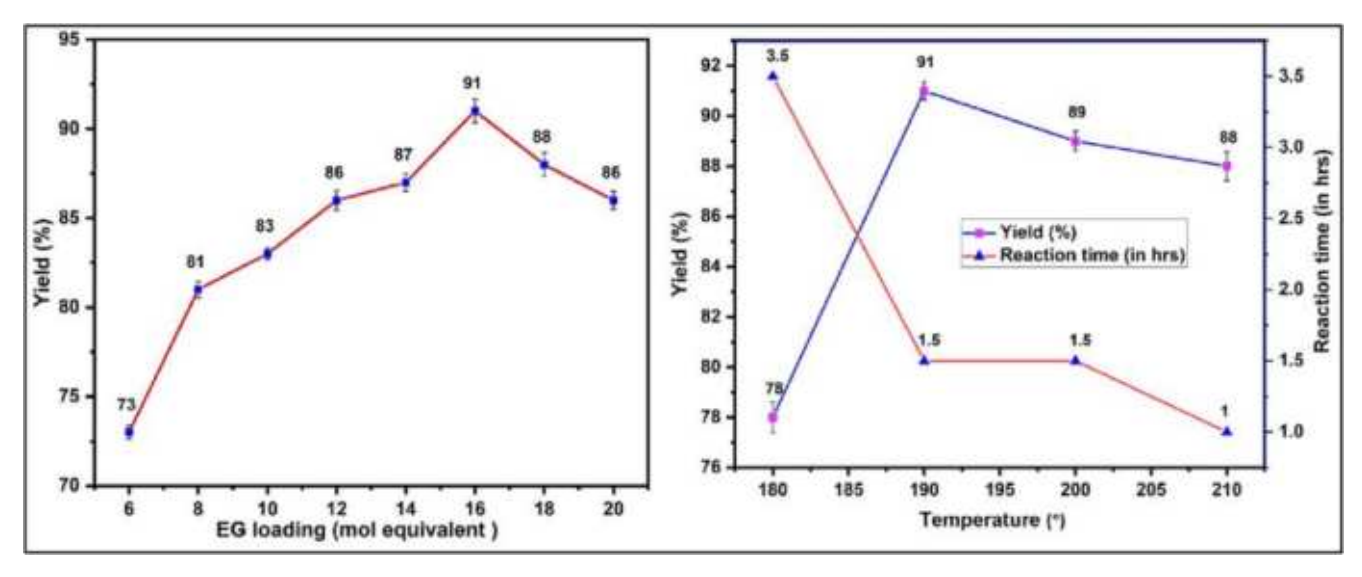
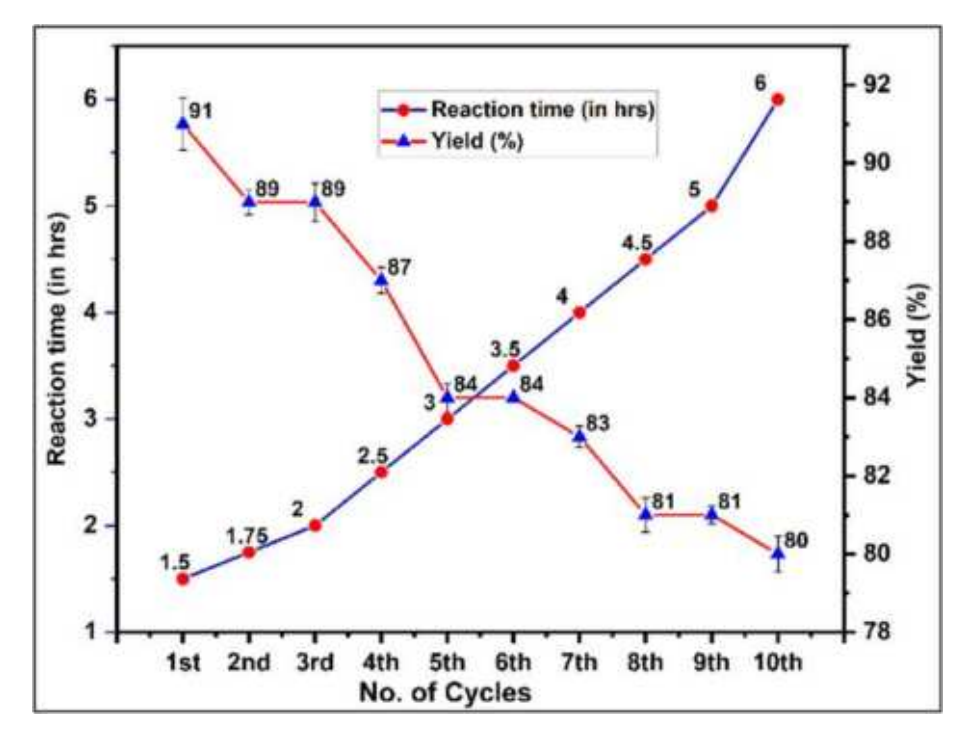


Fig. 7. (a) Optimization of reagent loading. Reaction condition: 2.5 mmol of PET flakes, 4 wt% catalyst, 1.5 hrs reaction time, at 190 °C. (b) Optimization of reaction temperature. Reaction condition: 2.5 mmol of PET flakes, 4 wt% catalyst, 16 equivalents of EG.



 $\textbf{Fig. 8.} \ \ \text{Reusability of OPA@Fe}_3O_4 \ \text{catalyst up to 10th catalytic cycles.} \ \ \text{Reaction condition: 2.5 mmol of PET flakes, 4 wt\% \ catalyst, 16 equivalents of EG, at 190 °C.}$

3.2.6. Reaction mechanism

The plausible reaction mechanism for the transesterification of PET through glycolysis using OPA@Fe $_3O_4$ catalyst was proposed via the general heterogeneous catalytic pathway,[42,57] and is shown in Scheme 1. In heterogeneous catalysis, the reactants disseminate onto the surface of the catalyst and get absorbed with the formation of new bonds. The reacting molecules then interact with each other to form new products, followed by desorption from the surface of the catalyst to give the isolated final products. As already mentioned above, analysis of the catalyst acknowledges the presence of high content of basic metal oxides of potassium (K) and calcium (Ca), and thus, we consider the catalytic action of oxides of potassium (K $_2O$) and calcium (CaO) in the probable reaction mechanism. Initially, with the introduction of

the catalyst, the oxygen anions (O^{2-}) from the catalyst basically executed the deprotonation of ethylene glycol, resulting in the formation of a nucleophilic 2-hydroxyethanolate ion. The generated nucleophile then attacks the electron deficient carbon atom of C = O from the ester of PET to form a tetrahedral intermediate. With the formation of a new C = O bond, the ester bond in the chain cleaved, which was followed by the disintegration of the PET polyester into its oligomers, dimers and then monomer. Meanwhile, the $-OCH_2CH_2$ - group from the initial PET chain acts as a leaving group and takes up the proton (H^+) from the catalyst to form $HOCH_2CH_2$ -. During glycolysis of PET, the generation of BHET proceeds through a reversible step-by-step reaction, creating an equilibrium between the oligomers, dimers and monomer. [43].

Scheme 1. Proposed mechanistic pathway for the glycolysis of PET.

3.3. Methanolysis reaction of PET waste

In an effort to amplify the scope and catalytic efficiency of the catalyst, methanolysis of PET polyester was also examined using a magnetic OPA@Fe₃O₄ catalyst. The formation of DMT was confirmed by performing ¹H NMR and ¹³C NMR analysis as shown in Figure S8 and S9 (see Supplementary Material Figure S8 and S9). In its ¹H NMR data, the recrystallized product showed one singlet at δ = 8.10 ppm from two aromatic protons and another singlet at δ = 3.94 ppm due to methoxy protons while its ¹³C NMR data exhibited peaks at δ = 166.27, 133.90, 129.55 and 52.43 ppm, validating the formation of the DMT monomer (see Supplementary Material Figure S9). Investigation of the FTIR spectra of the recrystallized product (see Supplementary Material Figure S10) displayed an absorption band at 1720 cm⁻¹ which reveals the presence of carbonyl groups of ester functionality. Also, the occurrence of strong absorption bands at 1262 and 1050 cm⁻¹ can be assigned to the ester C-O and C-O-C stretching vibrations.[74] And the observation of peaks at 1430 cm⁻¹ and 2965 cm⁻¹ indicates the presence of aromatic C-H and methyl group, respectively. Analysis of the crude product using High Performance Liquid Chromatography (HPLC) revealed the formation of EG, BHET, HEMT and DMT at a retention time of 1.953, 3.341, 4.445 and 7.908, respectively (Fig. 9). Investigation of commercially available EG, BHET, HEMT and DMT using HPLC was used to confirm the above observations.[40,41].

Despite the outstanding physicochemical identity of the nanosized catalyst, the production of DMT was also clearly affected by various operating reaction variables, such as duration of reaction, catalyst loading and methanol to PET concentration. Studies showed that DMT yield increases with increasing the reaction time, reaching a maximum at 1 hr with 79% yield, under a catalyst loading of 10 wt% and 5 mL of methanol at 200 °C (see Supplementary Material Table S3). However, prolonging the reaction time after 1 hr gradually decreases the percentage yield which may be due to the development of the reversible reaction.[39,41].

The influence of the catalyst loading on PET to DMT production was also investigated while keeping different reaction parameters such as reagent loading, reaction time and temperature constant at 5 mL, 1 hr and 200 °C, respectively (see Supplementary Material Table S4). Consequently, the best yield of 83% could be achieved when the catalyst loading was limited to 4 wt%. But, a further increment in the catalyst loading eventually decomposes the percentage yield after crossing the equilibrium condition. This can be explained due to the fact that after reaching the optimum value, transesterification reaction creates a chemical equilibrium between the reactants and product, which induces the equilibrium to shift towards the left side, thereby reducing the overall yield of

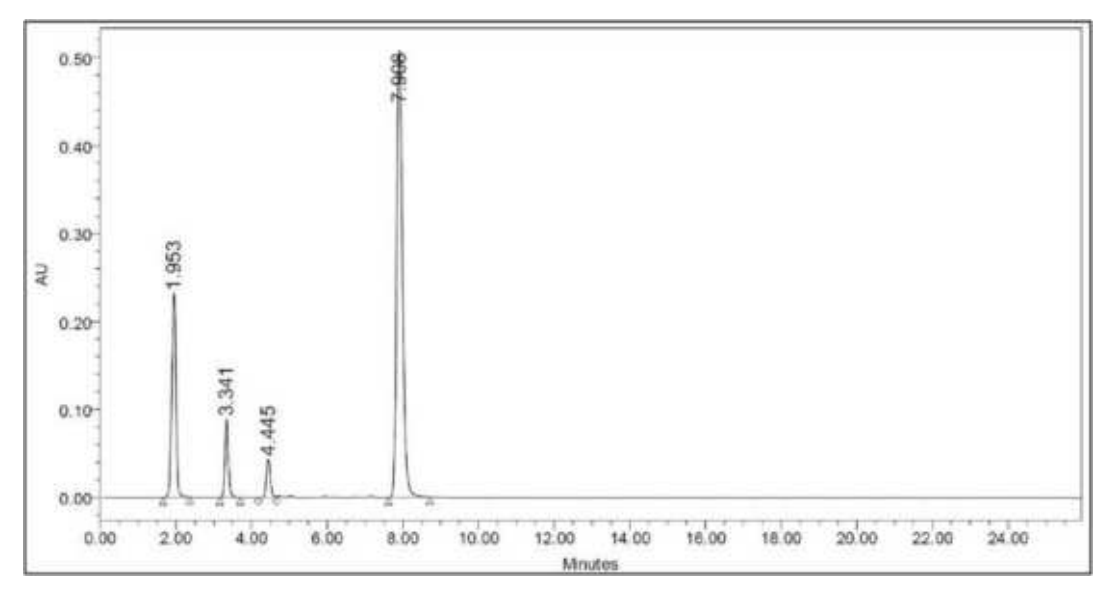


Fig. 9. HPLC analysis of the crude product.

the product.[38] Besides these, one of the principal factors determining the formation of the desired DMT monomer is methanol to PET ratio. As shown in Table S5 (see Supplementary Material Table S5), when methanol concentration was increased from 3 to 5 mL, DMT yield also jumped from 77% to 83%. However, further increase in methanol concentration beyond 5 mL doesn't have any remarkable effects on the product formation; instead, we observe a slight decreased in the percentage of yield.[35,42] So, after this examination, the optimum condition for methanolysis of PET granules using biomass waste-derived magnetic OPA@Fe₃O₄ was established at 2.5 mmol of PET flakes, 49 M equivalents of methanol (5 mL), a temperature of 200 °C and 1 hr reaction time.

The proposed reaction mechanism for methanolysis of PET is shown in Scheme S1 (see Supplementary Material Scheme S1) and is assumed to materialize through cation-anion combinatorial influence. And the oxides and carbonates of K and Ca present in the catalyst are believed to be the active sites for this transformation. Initially, high temperature and pressure and the presence of methanol inside the reactor vessel prompted the PET chain to be shortened by about 1/3.[38] The shortened PET chain then gets fragmented into the oligomers which was finally disintegrated into the monomers using the catalyst. The metal cations in the catalyst act as Lewis acid, which protonates the carbonyl oxygen of the ester functionality to intensify electrophilicity at the carbonyl carbon. Concurrently, the oxides of K and Ca abstract proton from methanol, promoting a nucleophilic attack from the oxygen atom of methanol to the electron rich carbonyl group. With the formation of a new C-O bond, the ester linkage breaks, subsequently forming DMT and EG as the final products. However, the process is reversible and as the reaction proceeds further, DMT and EG recombine to form BHET and HEMT as side products.

The efficacy of recovered magnetic OPA@Fe $_3O_4$ was also screened for the conversion of PET to DMT under the optimized controlled environment. After completion, the residual nanosized catalyst recovered using an external magnet was washed thoroughly with hot methanol. The recovered catalyst was dried at 80 °C for 12 hrs and then examined for the next ten consecutive cycles (see Supplementary Material Table S6). It was observed that there is a gradual decrease in the production yield after each run, but the catalyst was able to maintain an acceptable DMT yield even after ten cycles, achieving more than 70% DMT from the last runs. Reduced DMT production after each successive cycle may be sub-

jected to leaching of active sites or loss of surface area of the solid base catalyst,[75] which basically reduces its stability and reactivity.

4. Conclusion

In conclusion, the present study describes the preparation of orange peel ash coated magnetic nanoparticles and its utilization in the depolymerization of PET waste. The prepared catalyst, OPA@Fe₃O₄ was found to contain a high surface area, a highly mesoporous quality and a remarkable basic strength to show excellent catalytic performance with an excellent yield of BHET (91%) and DMT (83%) monomers under the optimized reaction conditions. Moreover, its magnetically retrievable characteristic makes it very easy to be recovered from the reaction medium and hence, was reused for a maximum of ten consecutive runs with a minor decline in its activities. The simplicity of the preparation procedure, easy handling and high efficacy of OPA@Fe₃O₄ catalyst provides a greener and economically feasible alternative method of PET depolymerization technique, furnishing its potential application at an industrial scale for the treatment of PET waste.

Declaration of Competing Interest

The authors declare that they have no known competing financial interests or personal relationships that could have appeared to influence the work reported in this paper.

Acknowledgements

The authors would like to thank Science and Engineering Research Board, New Delhi, India, File no. CRG/2022/000821 and File no EEQ/2017/000505 for financial support. We gratefully acknowledge SICART, SAIF-NEHU, BIT-Bangalore and IISc, Bangalore for sample analyses.

Appendix A. Supplementary material

Supplementary data to this article can be found online at https://doi.org/10.1016/j.apt.2023.104076.

References

- [1] A.L. Brooks, S. Wang, J.R. Jambeck, The Chinese import ban and its impact on global plastic waste trade, Sci. Adv. 4 (6) (2018).
- [2] A.R. Rahimi, J.M. Garciá, Chemical recycling of waste plastics for new materials production, Nat. Rev. Chem. 1 (2017), https://doi.org/10.1038/s41570-017-0046
- [3] European-Plastics An analysis of European plastics production, demand and waste data 2015.
- [4] O. Horodytska A. Cabanes A. Fullana Plastic Waste Management: Current Status and Weaknesses 2019 10.1007/698_2019_408.
- [5] C.M. Rochman, E. Hoh, B.T. Hentschel, S. Kaye, Long-term field measurement of sorption of organic contaminants to five types of plastic pellets: Implications for plastic marine debris, Environ. Sci. Technol. 47 (2013) 1646–1654, https:// doi.org/10.1021/es303700s.
- [6] D. Paszun, T. Spychaj, Chemical Recycling of Poly(ethylene terephthalate), 1997
- [7] K.R. Vanapalli, H.B. Sharma, V.P. Ranjan, B. Samal, J. Bhattacharya, B.K. Dubey, S. Goel, Challenges and strategies for effective plastic waste management during and post COVID-19 pandemic, Sci. Total Environ. 750 (2021) 141514.
- [8] K. Dutt, R.K. Soni, A review on synthesis of value added products from polyethylene terephthalate (PET) waste, Polym. Sci. - Ser. B 55 (2013) 430–452, https://doi.org/10.1134/S1560090413070075.
- [9] C. Jehanno, M.M. Pérez-Madrigal, J. Demarteau, H. Sardon, A.P. Dove, Organocatalysis for depolymerisation, Polym. Chem. 10 (2019) 172–186, https://doi.org/10.1039/c8py01284a.
- [10] Y.S. Parab, N.D. Pingale, S.R. Shukla, Aminolytic depolymerization of poly (ethylene terephthalate) bottle waste by conventional and microwave irradiation heating, J. Appl. Polym. Sci. 125 (2012) 1103–1107, https://doi. org/10.1002/app.34855.
- [11] H.I. Khalaf, O.A. Hasan, Effect of quaternary ammonium salt as a phase transfer catalyst for the microwave depolymerization of polyethylene terephthalate waste bottles, Chem. Eng. J. 192 (2012) 45–48, https://doi.org/10.1016/j. cej.2012.03.081.
- [12] R.K. Padhan, A. Sreeram, in: Recycling of Polyethylene Terephthalate Bottles, Elsevier, 2019, pp. 135–147.
- [13] M. Han, in: Recycling of Polyethylene Terephthalate Bottles, Elsevier, 2019, pp. 85–108.
- [14] A. Sheel, D. Pant, in: Recycling of Polyethylene Terephthalate Bottles, Elsevier, 2019, pp. 61–84.
- [15] R. López-Fonseca, I. Duque-Ingunza, B. de Rivas, L. Flores-Giraldo, J.I. Gutiérrez-Ortiz, Kinetics of catalytic glycolysis of PET wastes with sodium carbonate, Chem. Eng. J. 168 (2011) 312–320, https://doi.org/10.1016/j.cei.2011.01.031.
- [16] M. Ghaemy, K. Mossaddegh, Depolymerisation of poly(ethylene terephthalate) fibre wastes using ethylene glycol, Polym. Degrad. Stab. 90 (2005) 570–576, https://doi.org/10.1016/j.polymdegradstab.2005.03.011.
- [17] S.R. Shukla, K.S. Kulkarni, Depolymerization of poly(ethylene terephthalate) waste, J. Appl. Polym. Sci. 85 (2002) 1765–1770, https://doi.org/10.1002/app.10714.
- [18] K. Troev, G. Grancharov, R. Tsevi, I. Gitsov, A novel catalyst for the glycolysis of poly(ethylene terephthalate), J. Appl. Polym. Sci. 90 (8) (2003) 2301.
- [19] R. López-Fonseca, I. Duque-Ingunza, B. de Rivas, S. Arnaiz, J.I. Gutiérrez-Ortiz, Chemical recycling of post-consumer PET wastes by glycolysis in the presence of metal salts, Polym. Degrad. Stab. 95 (2010) 1022–1028, https://doi.org/ 10.1016/j.polymdegradstab.2010.03.007.
- [20] S.R. Shukla, V. Palekar, N. Pingale, Zeolite catalyzed glycolysis of polyethylene terephthalate bottle waste, J. Appl. Polym. Sci. 110 (2008) 501–506, https:// doi.org/10.1002/app.28656.
- [21] Q.F. Yue, C.X. Wang, L.N. Zhang, Y. Ni, Y.X. Jin, Glycolysis of poly(ethylene terephthalate) (PET) using basic ionic liquids as catalysts, Polym. Degrad. Stab. 96 (2011) 399–403, https://doi.org/10.1016/j.polymdegradstab.2010.12.020.
- [22] X. Zhou, X. Lu, Q. Wang, M. Zhu, Z. Li, Effective catalysis of poly(ethylene terephthalate) (PET) degradation by metallic acetate ionic liquids, Pure Appl. Chem. 84 (2012) 789–801, https://doi.org/10.1351/PAC-CON-11-06-10.
- [23] H. Wang, Z. Li, Y. Liu, X. Zhang, S. Zhang, Degradation of poly(ethylene terephthalate) using ionic liquids, Green Chem. 11 (2009) 1568–1575, https:// doi.org/10.1039/b906831g.
- [24] Q. Wang, Y. Geng, X. Lu, S. Zhang, First-row transition metal-containing ionic liquids as highly active catalysts for the glycolysis of poly(ethylene terephthalate) (PET), ACS Sustain. Chem. Eng. 3 (2015) 340–348, https://doi.org/10.1021/sc5007522.
- [25] Q. Wang, X. Lu, X. Zhou, M. Zhu, H. He, X. Zhang, 1-Allyl-3-methylimidazolium halometallate ionic liquids as efficient catalysts for the glycolysis of poly (ethylene terephthalate), J. Appl. Polym. Sci. 129 (2013) 3574–3581, https://doi.org/10.1002/app.38706.
- [26] A.M. Al-Sabagh, F.Z. Yehia, A.M.F. Eissa, M.E. Moustafa, G. Eshaq, A.M. Rabie, A. E. Elmetwally, Cu- and Zn-acetate-containing ionic liquids as catalysts for the glycolysis of poly(ethylene terephthalate), Polym. Degrad. Stab. 110 (2014) 364–377, https://doi.org/10.1016/j.polymdegradstab.2014.10.005.
- [27] A.M. Al-Sabagh, F.Z. Yehia, A.M.M.F. Eissa, M.E. Moustafa, G. Eshaq, A.R.M. Rabie, A.E. Elmetwally, Glycolysis of poly(ethylene terephthalate) catalyzed by the Lewis base ionic liquid [Bmim][OAc], Ind. Eng. Chem. Res. 53 (2014) 18443–18451, https://doi.org/10.1021/ie503677w.

- [28] C. Shuangjun, S. Weihe, C. Haidong, Z. Hao, Z. Zhenwei, F.u. Chaonan, Glycolysis of poly(ethylene terephthalate) waste catalyzed by mixed Lewis acidic ionic liquids, J. Therm. Anal. Calorim. 143 (5) (2021) 3489–3497.
- [29] Y. Liu, X. Yao, H. Yao, Q. Zhou, J. Xin, X. Lu, S. Zhang, Degradation of poly (ethylene terephthalate) catalyzed by metal-free choline-based ionic liquids, Green Chem. 22 (2020) 3122–3131, https://doi.org/10.1039/d0gc00327a.
- [30] L. Wang, G.A. Nelson, J. Toland, J.D. Holbrey, Glycolysis of PET using 1,3-Dimethylimidazolium-2-Carboxylate as an Organocatalyst, ACS Sustain. Chem. Eng. 8 (2020) 13362–13368, https://doi.org/10.1021/acssuschemeng.0c04108.
- [31] C. Jehanno, I. Flores, A.P. Dove, A.J. Müller, F. Ruipérez, H. Sardon, Organocatalysed depolymerisation of PET in a fully sustainable cycle using thermally stable protic ionic salt, Green Chem. 20 (2018) 1205–1212, https://doi.org/10.1039/c7gc03396f.
- [32] M. Genta, T. Iwaya, M. Sasaki, M. Goto, Supercritical methanol for polyethylene terephthalate depolymerization: observation using simulator, Waste Manag. 27 (2007) 1167–1177, https://doi.org/10.1016/j.wasman.2006.06.005.
- [33] M. Goto, H. Koyamoto, A. Kodama, T. Hirose, S. Nagaoka, Depolymerization of polyethylene terephthalate in supercritical methanol, J. Phys. Condens. Matter 14 (2002) 11427–11430, https://doi.org/10.1088/0953-8984/14/44/494.
- [34] T. Sako, T. Sugeta, K. Otake, N. Nakazawa, M. Sato, K. Namiki, M. Tsugumi, Depolymerization of polyethylene terephthalate to monomers with supercritical methanol, J. Chem. Eng. Jpn. 30 (1997) 342–346, https://doi.org/10.1252/jcej.30.342.
- [35] Y. Yang, Y. Lu, H. Xiang, Y. Xu, Y. Li, Study on methanolytic depolymerization of PET with supercritical methanol for chemical recycling, Polym. Degrad. Stab. 75 (2002) 185–191, https://doi.org/10.1016/S0141-3910(01)00217-8.
- [36] A.B. Raheem, Z.Z. Noor, A. Hassan, M.K. Abd Hamid, S.A. Samsudin, A.H. Sabeen, Current developments in chemical recycling of post-consumer polyethylene terephthalate wastes for new materials production: a review, J. Clean. Prod. 225 (2019) 1052–1064, https://doi.org/10.1016/j.jclepro.2019.04.019.
- [37] M.N. Siddiqui, H.H. Redhwi, D.S. Achilias, Recycling of poly(ethylene terephthalate) waste through methanolic pyrolysis in a microwave reactor, J. Anal. Appl. Pyrolysis 98 (2012) 214–220, https://doi.org/10.1016/J. IAAP.2012.09.007.
- [38] H. Kurokawa, M.A. Ohshima, K. Sugiyama, H. Miura, Methanolysis of polyethylene terephthalate (PET) in the presence of aluminium tiisopropoxide catalyst to form dimethyl terephthalate and ethylene glycol, Polym. Degrad. Stab. 79 (2003) 529–533, https://doi.org/10.1016/S0141-3910
- [39] D.D. Pham, J. Cho, Low-energy catalytic methanolysis of poly (ethyleneterephthalate), Green Chem. 23 (2021) 511–525, https://doi.org/ 10.1039/d0gc03536j.
- [40] S. Lalhmangaihzuala, Z. Laldinpuii, C. Lalmuanpuia, K. Vanlaldinpuia, Glycolysis of poly(Ethylene terephthalate) using biomass-waste derived recyclable heterogeneous catalyst, Polymers (Basel) 13 (2021) 1–13, https://doi.org/10.3390/polym13010037.
- [41] Z.T. Laldinpuii, V. Khiangte, S. Lalhmangaihzuala, C. Lalmuanpuia, Z. Pachuau, C. Lalhriatpuia, K. Vanlaldinpuia, Methanolysis of PET waste using heterogeneous catalyst of bio-waste origin, J. Polym. Environ. 30 (2022) 1600–1614, https://doi.org/10.1007/s10924-021-02305-0.
- [42] Z.T. Laldinpuii, C. Lalmuanpuia, S. Lalhmangaihzuala, V. Khiangte, Z. Pachuau, K. Vanlaldinpuia, Biomass waste-derived recyclable heterogeneous catalyst for aqueous aldol reaction and depolymerization of PET waste, New J. Chem. 45 (2021) 19542–19552, https://doi.org/10.1039/d1nj03225a.
- [43] Z. Laldinpuii, S. Lalhmangaihzuala, Z. Pachuau, K. Vanlaldinpuia, Depolymerization of poly(ethylene terephthalate) waste with biomass-waste derived recyclable heterogeneous catalyst, Waste Manag. 126 (2021) 1–10, https://doi.org/10.1016/j.wasman.2021.02.056.
- [44] A.S. Teja, P.Y. Koh, Synthesis, properties, and applications of magnetic iron oxide nanoparticles, Prog. Cryst. Growth Charact. Mater. 55 (2009) 22–45, https://doi.org/10.1016/j.pcrysgrow.2008.08.003.
- [45] K. Rajkumari, J. Kalita, D. Das, L. Rokhum, Magnetic Fe3O4@silica sulfuric acid nanoparticles promoted regioselective protection/deprotection of alcohols with dihydropyran under solvent-free conditions, RSC Adv. 7 (2017) 56559– 56565. https://doi.org/10.1039/c7ra12458a.
- [46] S. Singamaneni, V.N. Bliznyuk, C. Binek, E.Y. Tsymbal, Magnetic nanoparticles: recent advances in synthesis, self-assembly and applications, J. Mater. Chem. 21 (2011) 16819–16845, https://doi.org/10.1039/c1jm11845e.
- [47] S. Abdolmohammadi, S. Shariati, N.E. Fard, A. Samani, Aqueous-Mediated green synthesis of novel spiro[indole-quinazoline] derivatives using kit-6 mesoporous silica coated Fe3O4 nanoparticles as catalyst, J. Heterocycl. Chem. 57 (2020) 2729–2737, https://doi.org/10.1002/jhet.3981.
- [48] A. Moussa, A. Rahmati, Synthesis and characterization of silica-coated Fe3O4 nanoparticle@silylpropyl triethylammonium polyoxometalate as an organic-inorganic hybrid heterogeneous catalyst for the one-pot synthesis of tetrahydrobenzimidazo[2,1-b]quinazolin-1(2H)-ones, Appl. Organomet. Chem. 34 (2020), https://doi.org/10.1002/aoc.5894.
- [49] A.A. Barzinjy, D.A. Abdul, F.H.S. Hussain, S.M. Hamad, Green synthesis of the magnetite (Fe3O4) nanoparticle using Rhus coriaria extract: a reusable catalyst for efficient synthesis of some new 2-naphthol bis-Betti bases, lnorg. Nano-Metal Chem. 50 (2020) 620–629, https://doi.org/10.1080/ 24701556.2020.1723027.
- [50] M.R. Mehrasbi, J. Mohammadi, M. Peyda, M. Mohammadi, Covalent immobilization of Candida antarctica lipase on core-shell magnetic

- nanoparticles for production of biodiesel from waste cooking oil, Renew. Energy 101 (2017) 593–602, https://doi.org/10.1016/j.renene.2016.09.022.
- [51] Zillillah, T.A. Ngu, Z. Li, Li, Phosphotungstic acid-functionalized magnetic nanoparticles as an efficient and recyclable catalyst for the one-pot production of biodiesel from grease via esterification and transesterification, Green Chem. 16 (3) (2014) 1202.
- [52] Y. Liu, P. Zhang, M. Fan, P. Jiang, Biodiesel production from soybean oil catalyzed by magnetic nanoparticle MgFe2O4@CaO, Fuel 164 (2016) 314–321, https://doi.org/10.1016/j.fuel.2015.10.008.
- [53] S. Amirnejat, A. Nosrati, S. Javanshir, Superparamagnetic Fe3O4@Alginate supported L-arginine as a powerful hybrid inorganic-organic nanocatalyst for the one-pot synthesis of pyrazole derivatives, Appl. Organomet. Chem. 34 (2020), https://doi.org/10.1002/aoc.5888.
- [54] A.M. Al-Sabagh, F.Z. Yehia, D.R.K. Harding, G. Eshaq, A.E. ElMetwally, Fe3O4-boosted MWCNT as an efficient sustainable catalyst for PET glycolysis, Green Chem. 18 (2016) 3997–4003, https://doi.org/10.1039/c6gc00534a.
- [55] I. Cano, C. Martin, J.A. Fernandes, R.W. Lodge, J. Dupont, F.A. Casado-Carmona, R. Lucena, S. Cardenas, V. Sans, I. de Pedro, Paramagnetic ionic liquid-coated SiO2@Fe3O4 nanoparticles—the next generation of magnetically recoverable nanocatalysts applied in the glycolysis of PET, Appl. Catal. B 260 (2020) 118110, https://doi.org/10.1016/j.apcatb.2019.118110.
- [56] M.R. Nabid, Y. Bide, M. Jafari, Boron nitride nanosheets decorated with Fe3O4 nanoparticles as a magnetic bifunctional catalyst for post-consumer PET wastes recycling, Polym. Degrad. Stab. 169 (2019) 108962, https://doi.org/10.1016/j.polymdegradstab.2019.108962.
- [57] B. Changmai, R. Rano, C. Vanlalveni, S.L. Rokhum, A novel Citrus sinensis peel ash coated magnetic nanoparticles as an easily recoverable solid catalyst for biodiesel production, Fuel 286 (2021) 119447, https://doi.org/10.1016/ if nel 2020 119447
- [58] M.K. Kumawat, S.L. Rokhum, Biodiesel production from oleic acid using biomass-derived sulfonated orange peel catalyst, Front. Catal. 2 (2022) 13, https://doi.org/10.3389/FCTLS.2022.914670.
- [59] A. Lopez-Santiago, H.R. Grant, P. Gangopadhyay, R. Voorakaranam, R.A. Norwood, N. Peyghambarian, Cobalt ferrite nanoparticles polymer composites based all-optical magnetometer, Opt. Mater. Express 2 (7) (2012) 978
- [60] K. Rajkumari, B. Changmai, A.K. Meher, C. Vanlalveni, P. Sudarsanam, A.E.H. Wheatley, S.L. Rokhum, A reusable magnetic nanocatalyst for bio-fuel additives: the ultrasound-assisted synthesis of solketal, Sustain. Energy Fuels 5 (2021) 2362–2372, https://doi.org/10.1039/DOSE01900C.
- [61] M. Balajii, S. Niju, Banana peduncle a green and renewable heterogeneous base catalyst for biodiesel production from Ceiba pentandra oil, Renew. Energy 146 (2020) 2255–2269, https://doi.org/10.1016/j.renene.2019.08.062.
- [62] M. Gohain, A. Devi, D. Deka, Musa balbisiana Colla peel as highly effective renewable heterogeneous base catalyst for biodiesel production, Ind. Crops Prod. 109 (2017) 8–18, https://doi.org/10.1016/j.indcrop.2017.08.006.
- [63] S. Vasantharaj, S. Sathiyavimal, P. Senthilkumar, F. LewisOscar, A. Pugazhendhi, Biosynthesis of iron oxide nanoparticles using leaf extract of

- Ruellia tuberosa: antimicrobial properties and their applications in photocatalytic degradation, J. Photochem. Photobiol. B 192 (2019) 74–82, https://doi.org/10.1016/j.jphotobiol.2018.12.025.
- [64] A.P.S. Chouhan, A.K. Sarma, Biodiesel production from Jatropha curcas L. oil using Lemna perpusilla Torrey ash as heterogeneous catalyst, Biomass Bioenergy 55 (2013) 386–389, https://doi.org/10.1016/j.biombioe.2013.02.009.
- [65] K.S.W. Sing, R.T. Williams, Physisorption hysteresis loops and the characterization of nanoporous materials, Adsorpt. Sci. Technol. 22 (2004) 773–782, https://doi.org/10.1260/0263617053499032.
- [66] M. Imran, K.G. Lee, Q. Imtiaz, B.K. Kim, M. Han, B.G. Cho, D.H. Kim, Metal-oxide-doped silica nanoparticles for the catalytic glycolysis of polyethylene terephthalate, J. Nanosci. Nanotechnol. 11 (2011) 824–828, https://doi.org/10.1166/jnn.2011.3201.
- [67] C. Liu, J. Yuan, H. Gao, C. Liu, Biodiesel production from waste cooking oil by immobilized lipase on superparamagnetic Fe3O4 hollow sub-microspheres, Biocatal. Biotransform. 34 (2016) 283–290, https://doi.org/10.1080/ 10242422.2016.1265948.
- [68] G. Xi, M. Lu, C. Sun, Study on depolymerization of waste polyethylene terephthalate into monomer of bis(2-hydroxyethyl terephthalate), Polym. Degrad. Stab. 87 (2005) 117–120, https://doi.org/10.1016/j. polymdegradstab.2004.07.017.
- [69] S.H. Shuit, S.H. Tan, Biodiesel Production via Esterification of Palm Fatty Acid Distillate Using Sulphonated Multi-walled Carbon Nanotubes as a Solid Acid Catalyst: Process Study, Catalyst Reusability and Kinetic Study, Bioenergy Res. 8 (2015) 605–617. https://doi.org/10.1007/s12155-014-9545-2
- [70] D. Kumar, A. Ali, Transesterification of low-quality triglycerides over a Zn/CaO heterogeneous catalyst: kinetics and reusability studies, Energy Fuel 27 (2013) 3758–3768, https://doi.org/10.1021/EF400594T.
- [71] M. Gohain, K. Laskar, A.K. Paul, N. Daimary, M. Maharana, I.K. Goswami, A. Hazarika, U. Bora, D. Deka, Carica papaya stem: a source of versatile heterogeneous catalyst for biodiesel production and C-C bond formation, Renew. Energy 147 (2020) 541–555, https://doi.org/10.1016/j.renene.2019.09.016.
- [72] G. Boskovic, M. Baerns, Catalyst deactivation, Springer Ser. Chem. Phys. 75 (2004) 477–503, https://doi.org/10.1007/978-3-662-05981-4_14.
- [73] K. Fukushima, O. Coulembier, J.M. Lecuyer, H.A. Almegren, A.M. Alabdulrahman, F.D. Alsewailem, M.A. McNeil, P. Dubois, R.M. Waymouth, H. W. Horn, J.E. Rice, J.L. Hedrick, Organocatalytic depolymerization of poly (ethylene terephthalate), J. Polym. Sci. A Polym. Chem. 49 (2011) 1273–1281, https://doi.org/10.1002/POLA.24551.
- [74] J.T. Du, Q. Sun, X.F. Zeng, D. Wang, J.X. Wang, J.F. Chen, ZnO nanodispersion as pseudohomogeneous catalyst for alcoholysis of polyethylene terephthalate, Chem. Eng. Sci. 220 (2020), https://doi.org/10.1016/J.CES.2020.115642.
- [75] N. Kaur, A. Ali, Kinetics and reusability of Zr/CaO as heterogeneous catalyst for the ethanolysis and methanolysis of Jatropha crucas oil, Fuel Process. Technol. 119 (2014) 173–184, https://doi.org/10.1016/j.fuproc.2013.11.002.